Memoirs of the Faculty of Engineering, Okayama University, Vol. 43, pp. 61-74, January 2009

Human Interface Technology for Operation Support of Large Sized Crane

Mao KAWAMURA *
Dept. of Electrical and Electronic Engineering
Okayama University
3-1-1, Tsushima-Naka Okayama, 700-8530

Masami KONISHI
Dept. of Electrical and Electronic Engineering
Division of Industrial Innovation Science
The Graduate School of Natural Science and Technology
Okayama University
3-1-1, Tsushima-Naka Okayama, 700-8530

Katuki YAMAGATA
Kobelco Cranes co., Ltd
740 Yagi, Okubo, Akashi, Hyougo, Japan

Koichi SHIMOMURA
Kobelco Cranes co., Ltd
740 Yagi, Okubo, Akashi, Hyougo, Japan

(Received November 23, 2008)

In this research, a Human Interface system is designed intended to mobile crane. The intervention of human is unavoidable to attain the high performance of electro mechanical system. As is known, crane operation is complicated. Recently, the decrease of expert person induced crane accident. So in near future, it is required a partial automation of crane operation and human support technology. We are aiming at the development of the operation support system for a crane. In this research, development of the hydro mechanical models representing both of static and dynamics movements are made. Further, actual experimental data of operating mobile crane, which are electrical signal data and three-dimension (3D) position of moving load is measured. The actual operating data are compared with the model and it is found that the developed electromechanical model can explain the behaviors of actual data.

1 INTRODUCTION

Heretofore, industrial crane plays an important role as the effective machine to carry heavy load and large-figured object in the manufacturing premise, the construction field and so on. There are circling of the hanging load and boom hoisting in the operation of a crane. These operations are combined and the hanging load is carried to the destination. The operation of a crane requires the simultaneous operations of two or more levers and pedals for one movement, and operator must consider turbulences such as load swinging and wind in operation. Although recent crane seeks safety operation by using mechatronics and improvement of operation, there exists the possibility that an accident may occur during crane work. Crane operation is much complicated and highly depends on expert's experiences and skills. Recently, the decrease of expert persons caused crane accident. So, it is needed to realize the partial automation of crane operation and the support technology to reduce operating items.

*E-mail:kawamura@cntr.elec.okayama-u.ac.jp

We are aiming at the development of the support system for the crane operation preventing an industrial accident by this system. Our research is focused on a mobile crane. The schematic of mobile crane is shown in Fig.1. In this paper, it is shown the construction of simulation model for mobile crane combined with hydraulic model are designed. Hydraulic simulation data are compared with experiment data, and module parameter are identified using optimization algorithm. Finally, the concluding remark and future works are stated.

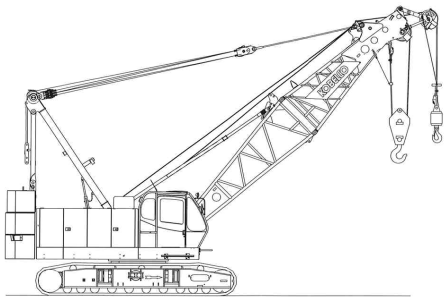

Fig. 1 Schematic of mobile cran

2 MEASUREMENT OF MOVING LOAD POSITION IN STEREO CAMERA

It can be said that the visual sense which in human's sensory body account for 87 percent of the recognition of external condition. It is most important sensory body for recognition of environment. So, it would appear that using the visual information that contains a lot of information to measure and to control the machine is able to construct an advanced system which can adapt to environmental changes.

The crane operator must consider turbulences such as load swinging and wind in operation. To understand operations by human, it is necessary to measure load position data and lever operation at the same time. Therefore, we constructed measurement system which is based on the method of stereo vision as the means of the measurement.

2.1 Calculation Procedure

Here, the measurement method of assuming the hanging load of the crane is described.

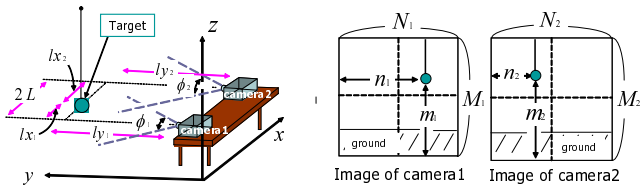

Fig. 2 Experimental image of stereo camera

Fig. 3 Target position are photographic image

As shown in Fig.2, two cameras are set up and each distance of axial direction are named lx, ly. Next, the coordinates of the target object of each camera shot are defined with $(n_1,\ m_1)$, $(n_2,\ m_2)$. N_1 and N_2 are pixel counts on the side of the main body of the camera, M_1 and M_2 are pixel counts on the vertical side. Thus, the following equations are described.

$$lx_1 = ly_1 \tan\frac{\phi_1}{2}[\frac{2n_1}{N_1} - 1] \tag{1}$$

$$lx_2 = ly_2 \tan\frac{\phi_2}{2}[1 - \frac{2n_2}{N_2}] \tag{2}$$

As the constraints,

$$lx_1 + lx_2 = 2L \tag{3}$$

$$ly_1 = ly_2. \tag{4}$$

Here, Eqs.(1) and (2) are transformed as follows.

$$a_1 = \tan\frac{\phi_1}{2}[\frac{2n_1}{N_1} - 1], a_2 = \tan\frac{\phi_2}{2}[1 - \frac{2n_2}{N_2}] \tag{5}$$

The Eqs.(1) to (4) are trasformed as follows.

$$lx_1 - [a_1]ly_1 = 0 \tag{6}$$

$$lx_2 - [a_2]ly_2 = 0 \tag{7}$$

$$lx_1 + lx_2 = 2L \tag{8}$$

$$ly_1 - ly_2 = 0 \tag{9}$$

These equations are converted in matrix form and described as in equation(10).

$$\begin{bmatrix} 1 & 0 & -a_1 & 0 \\ 0 & 1 & 0 & -a2 \\ 1 & 1 & 0 & 0 \\ 0 & 0 & 1 & -1 \end{bmatrix} \begin{bmatrix} lx_1 \\ lx_2 \\ ly_1 \\ ly_2 \end{bmatrix} = \begin{bmatrix} 0 \\ 0 \\ 2L \\ 0 \end{bmatrix} \tag{10}$$

Therefore, l_x, l_y are able to be calculated. Next, the height of the target object is determined as equations(11) and (12) from obtained value data.

$$z_1 = 2ly_1 \tan\frac{\phi_1}{2} \times \frac{M_1}{N_1} \times \frac{240 - m_1}{M_1} + L_{z1} \tag{11}$$

$$z_2 = 2ly_2 \tan\frac{\phi_2}{2} \times \frac{M_2}{N_2} \times \frac{240 - m_2}{M_2} + L_{z2} \qquad (12)$$

L_{z1} and L_{z2} are the heights of the cameras from ground. Camera shots of experiments that were conducted are shown in Fig.4 and 5.

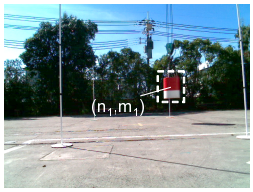

Fig. 4 Image of camera♯1

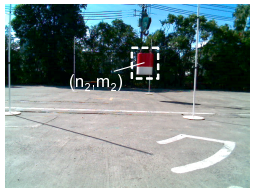

Fig. 5 Image of camera♯2

2.2 Method of Recognition of Target Object

Here, the method of recognizing the target object, used for the image data processing is described. This time, we employ the background subtraction to get coordinate point of hanging load. And, the algorithm was improved to speed up the data processing will be described.

2.2.1 Acquisition of Coordinates Point with Background Subtraction Image Processing

Application of a suitable background subtraction algorithm is a useful technique for correcting image defects that are associated with nonuniform brightness. First, background image and imput image which is taken stereo camera is changed to binary by some threshold amount. Example results are shown in Figs.6 and 7.

Fig. 6 Difference image(left) and imput image(right)

Fig. 7 Difference image

From Fig.7, it is confirmed that almost the noises other than hanging load is filtered out. But, the hook and the shadow are remained in the image. So, it is changed to binary by using the HLS conversion as a preprocessing for red color. The result is shown in the following.

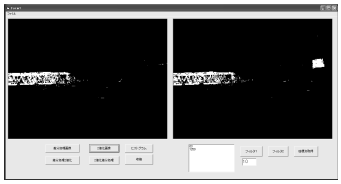

Fig. 8 Image binarization of difference image(left) and imput image(right)

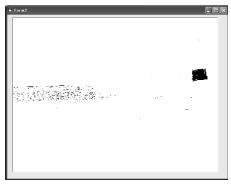

Fig. 9 Difference picture after making to binary is processed

As explained above, the hanging load part was able to be extracted. But, the noise has not been completely removed as shown in Fig.9. This reason is that a slight misalignment of camera was raised with the passage of time and the vibration, etc. For example, the vibration when the crane moves the hanging load is enumerated. Then, the contraction and the expansion filter are applied to this difference picture. The contraction and the expansion filter are described as follows.

Expansion filter

The expansion filter is the processing that replace the brightness of a center pixel of 3 × 3 with the maximal brightness in surrounding nine pixels (a center pixel is included).

Contraction filter

The contraction filter is the processing that replace the brightness of a center pixel of 3 × 3 with minimum brightness in surrounding nine pixels (a center pixel is included) contrary to the expansion.

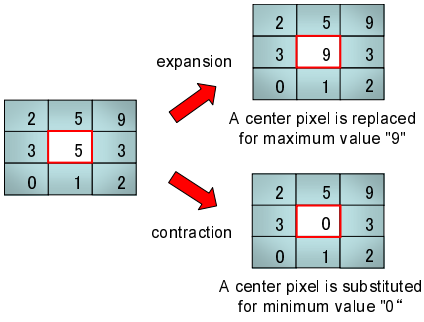

Fig. 10 Schematic diagram of 3 × 3-pixel filter

Therefore, when the input image is made to binarry and 1-pixel is assumed to be an object part and 0-pixel is assumed to a background pixel, it is described

as follows.

Expansion : processing that makes 1-pixel thick by 1-layer

If there is as much as one 1-pixel eight-neighborhoods of the note pixel, the note pixel is replaced by the note pixel with 1-pixel.

Contraction : processing that makes 1-pixel thin by 1-layer

If there is as much as one 0-pixel eight-neighborhoods of the note pixel, the note pixel is replaced by the note pixel with 0-pixel.

In this case, the noise is removed by using such an expansion and a contraction filter when the noise element is broken into the image. So, the coordinate point of the hanging load is identified when the shrinkage filter described in the above-mentioned is applied to this difference picture as follows.

Fig. 11 Acquisition of coordinates point

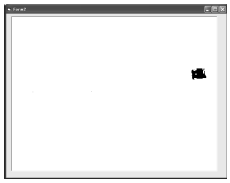

Fig. 12 Shrinkage processing of difference picture

2.2.2 Image Binarization

To simplify the calculation processing, the input image is made binary. The method is described as follows.

• YCC color space

In the signal of the color television, the brightness signal and the color signal are separated to have interchangeability with the black and white set and it is made. These signals, R(red), G(green), B(blue) are shown in eqation (13).

$$\left.\begin{aligned} Y &= 0.299R + 0.587G + 0.114B \\ C_1 &= R - Y = 0.701R - 0.587G - 0.114B \\ C_2 &= B - Y = -0.299R - 0.587G - 0.866B \end{aligned}\right\} \quad (13)$$

Y of eqation (13) shows the radiance value (brightness, brightness). Moreover,C_1 and C_2 of color information are shape to pull brightness signal Y from R and B respectively, and it is called the color-difference signal.

• HLS color space

When the color is expressed, the nuance is different depending on the individual. So, the following three elements are useful techniques for the quantitatively define.

Hue : The element that shows kind of colors such as R, G, B.

Light : The element that shows brightness, it corresponds to the concentration value of a monochrome image.

Saturation:The element that shows the color vividness, it becomes 0 in the achromatic color(black-ash-white).

These are called three attributes. Hue (H) is defined as follows.

$$H = \tan^{-1}\left(\frac{C_1}{C_2}\right) \quad (14)$$

L (light) is equal to Y of eqation (13), and S (saturation) is defined as a distance from a center axis (brightness L) and is described as follows.

$$S = \sqrt{C_1^2 + C_2^2} \quad (15)$$

To convert the image actually taken in HLS, to install the threshold, and to extract red in the side, it is made to binary. The original picture image is shown in Fig.13 and the image of binary is shown in Fig.14. In processing of image binarization, the threshold amounts are $H > 70, S > 60, R > G > B$ where the black is assumed to be 1 and the white is assumed to be 0.

Fig. 13 Original image

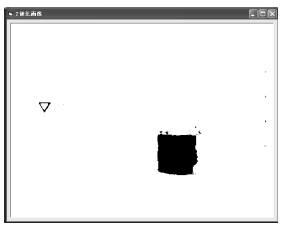

Fig. 14 Image binarization

2.2.3 Technology of Clipping Image of Target Object

Fig.15 shows he schematic of stereo camera and Fig.16 shows and the photographic image. The snap shot is

taken at the intervals of 0.1 seconds and their analyzed. As shown in Fig.15, first, a snap shot is taken with stereo camera[1]. Next, the image which is taken with stereo camera is handled to binarization, based on the color of the target objec in the image processing equipment[2], the back ground image is limited for the calculation processing speed-up in the equipment of clipping background image[3]. Then, the range limit with the equipment of clipping background image in the image projection equipment[4] is calculated. Finally, the recognition result is output.

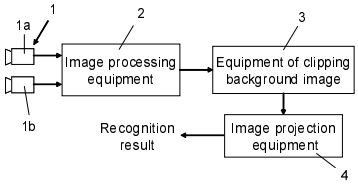

Fig. 15 Schematic diagram of stereo camera

Fig. 16 Photographic image with stereo camera

2.3 Calibration Technology of Pair Stereo Cameras

Here, three dimension coordinates acquisition equipment that is able to do the calibration of the stereo camera without need of a special device is described. It is difficult to set up each camera accurately along the axis of coordinate when the stereo camera is applied to an actual crane. Moreover, it can not be avoided the cause of a slight misalignment in the direction of the camera by a change with the passage of time and the vibration, etc. Therefore, it causes a significant error between the analyzed result and the actual crane's load position. So, we provide further insights into the correction technology of the measuring error that used the rotating transformation matrix and the optimization method for solving the problem. The correction technology, which is set the criterial object caught by each camera, and identify value of misalignment from the idealized state. The simulated annealing (SA) method was used for the optimization method.

2.3.1 Roll-Pitch-Yaw Matrix

This expression method expresses the posture after it rotates in the class of $RPY(\theta_r, \theta_p, \theta_y)$. As shown

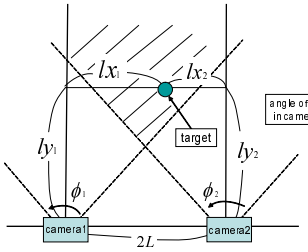

Fig. 17 Ideal condition

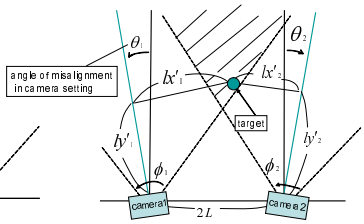

Fig. 18 Nonideal condition

in Fig.19, the angle of the gyration around z axis is called "Roll"(θ_r), the angle of the vertical movement around y is called "Pitch"(θ_p), and the angle of the side movement around y is called "Yaw"(θ_y),

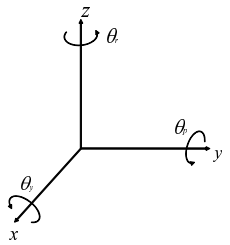

Fig. 19 Roll-Pitch-Yaw rotation

2.3.2 Rotating Coordinate Transformation

In Fig.20 ,the rotation transformation matrix of coordinate is asuumed $R(z, \theta)$ which was rotated around z axis and it is described as follows.

$$R(z,\theta) = \begin{bmatrix} \cos\theta & -\sin\theta & 0 \\ \sin\theta & \cos\theta & 0 \\ 0 & 0 & 1 \end{bmatrix} \tag{16}$$

By the same token, when the rotation transformation matrix which was rotated around y is assumed $R(y, \theta)$ and the rotation transformation matrix which was rotated around x is assumed $R(x, \theta)$, they are described as follows.

$$R(y,\theta) = \begin{bmatrix} \cos\theta & 0 & \sin\theta \\ 0 & 1 & 0 \\ -\sin\theta & 0 & \cos\theta \end{bmatrix} \tag{17}$$

$$R(x,\theta) = \begin{bmatrix} 1 & 0 & 0 \\ 0 & \cos\theta & -\sin\theta \\ 0 & \sin\theta & \cos\theta \end{bmatrix} \tag{18}$$

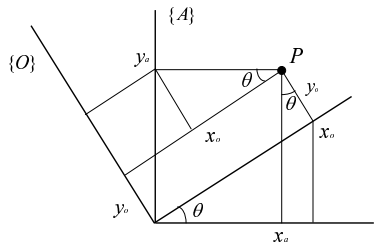

$$x_a = x_o \cdot \cos\theta - y_o \cdot \sin\theta$$
$$y_a = x_o \cdot \sin\theta + y_o \cdot \cos\theta$$

Fig. 20 Rotating coordinate transformation

Each parameter of angle is rotational transform angle. As well as the Roll-Pitch-Yaw rotation, these each rotating matrix is put together in Fig.19. The Roll angle is assumed to be θ_r, the Pitch angle is θ_p, the Yaw angle is θ_r, then the synthesis of the rotation transformation matrix is shown in equation (19).

$$RPY(\theta_r, \theta_p, \theta_y) = R(z, \theta_r) \cdot R(y, \theta_p) \cdot R(x, \theta_y) \quad (19)$$

2.3.3 Formulation to Optimization Problem

The point to understand the position will be called a reference position. A coordinate point of reference posistion is X, a coordinate point of analytic value with stereo camera is X', the value X'' is the rotated convert of X'. Then the optimization problem is shown as follows.

$$\min J$$
$$J = |X - X''| \quad (20)$$
$$\text{subject to} \quad X'' = F(\Delta\theta_r, \Delta\theta_p, \Delta\theta_y) \cdot X' \quad (21)$$

Here, $(\Delta\theta_r, \Delta\theta_p, \Delta\theta_y)$ are misaligement angles of the camera in each axis. $F(\Delta\theta_r, \Delta\theta_p, \Delta\theta_y)$ shows the rotation transformation matrix of equation (19).

Fig.22 shows the schematic diagram of calibration technology of pair stereo camera. The reference position is stored in the location information equipment[4]. Next, stereo processing is executed in the stereo processing equipment[2], and three dimension position is determined.

Then, to minimize the errors of actual reference position and calculated location information, optimization is executed. The amount of misalignment angle and moved distance that each camera are calculated. And, the calculated parameter is corrected with rotation coordinates parameter correcting equipment[5] and send it back to the stereo processing equipment[2].

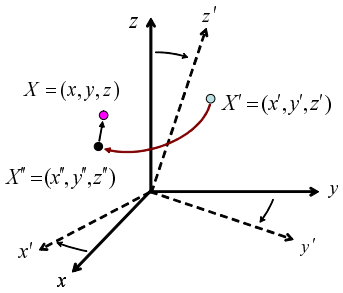

X: Reference position X': Analytic value with stereo camera

X'': Vector of procession after-rotation transform

Fig. 21 Three dimension rotation coordinate transformation

Finally, that is executed at regular intervals, and prevent the deterioration in change with the passage of time.

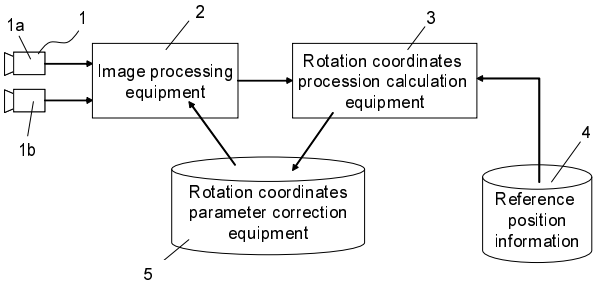

Fig. 22 Schematic diagram of calibration technology of Pair Stereo Camera

2.4 Confirmatory Experiment

The measuring experiment of the target object that assumed the hanging load was conducted with calibration technology of stereo camera. Experimental conditions, the experiment result, and discussion are described in the following.

2.4.1 Composition and Condition of Experimental Apparatus

Here, the experimental conditions are explained. As shown in Fig.23, the experiment that cameras are placed on the desk and the object which is assumed to be hanging load is hang from the ceiling in the laboratory is made.

First, the distance from the camera to target object is fixed in the 1.5m to 4.5m range, and the analytic value from stereo camera is compared with the actual position before calibration and after it to confirm the improvement of accuracy by the correction. Next, it leaves uniformly space from stereo camera and it is moved in parallel to x axis. Then, the situation is taken as a picture at intervals of 0.1 seconds and analyzed. The situation of the experimental condition is shown in Fig.23 and the necessary parameters for position measurement are shown Table 1.

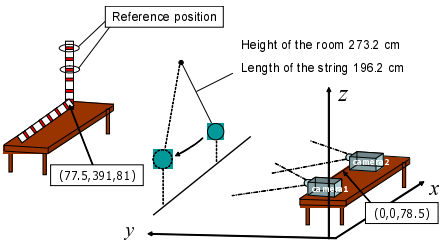

Fig. 23 Experiment condition

Table. 1 Parameter necessary for position measurement

Distance between cameras[$2L$]	100cm
Installation space[L_z]	78.5cm
View angle of camera1[ϕ_1]	61.08 °
View angle of camera2[ϕ_2]	61.51 °

2.4.2 Measurement of Static Target Object

The object which is hanging load was fixed and analysis was conducted to confirm utility of the proposal method. The analytic value from stereo camera is compared with the actual position before calibration and after it. The experiment results are shown in Fig.24.

In the present study, the acceptable range of error is set within $\pm$ 2 percent. From Fig.24, it is confirmed that the calibration technology meets this requirement.

2.4.3 Measurement of Dynamic Target Object

As shown in Fig.23, the object which is hanging load is moved along x-axis. Then, snap shot is taken as a picture as intervals of 0.1 seconds with stereo camera and analyze. The result and discussion are described as follows.

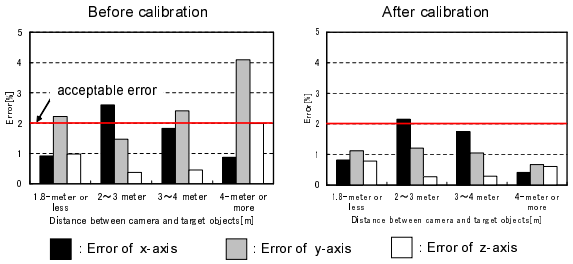

Fig. 24 Experimental result

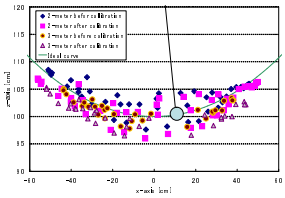

Fig. 25 Measurement of dynamic analysis

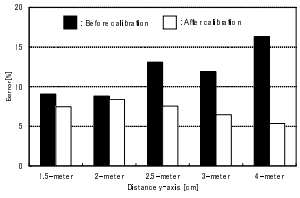

Fig. 26 Comparison of analytic value

Fig.25 is the result of viewing from the front. And, Fig.26 is the diagram that is comparison of the error of before calibration with the error after calibration.

From the above figure, it is confirmed utility of calibration technology, but the result showed exceeding 2 percent of the target precision. The cause is considered that the orbit of target object doesn't move parallel to x-axis, so the target object might be conducted an elliptical orbit. To prevent the situation, the object was forced to move parallel to the x-axis with transparent board, and repeated the same experiment. The result is shown as follows.

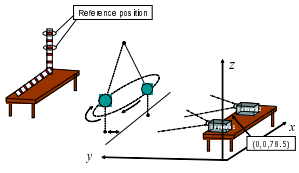

Fig. 27 Target boject moving in an elliptical orbit

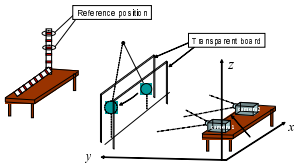

Fig. 28 Fixed orbit

It is confirmed that the orbit is improved by the calibration technology from in Figs.25 and 29. As compared Fig.26 with Fig.30, it is confirmed that the error has totally become small. For this, the orbit could not move parallel to x-axis. So, 2 percent of the target

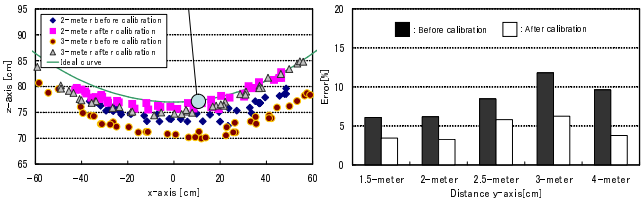

Fig. 29 Measurement of dynamic analysis

Fig. 30 Comparison of analytic value

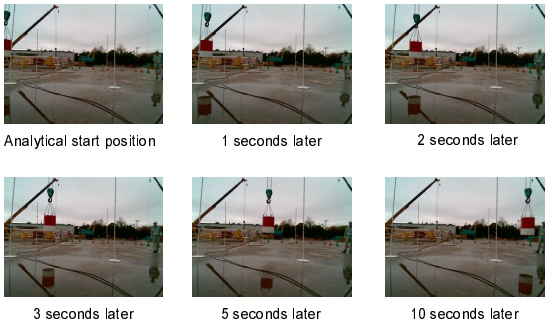

Fig. 33 Image of circling motion

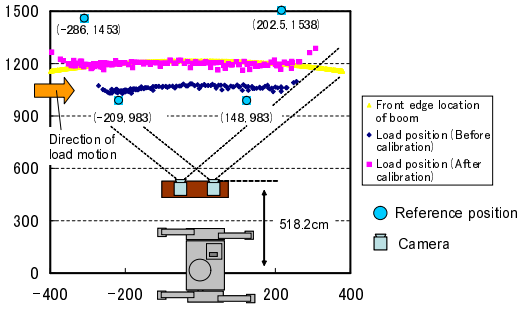

Fig. 34 Analyzed result of circling motion

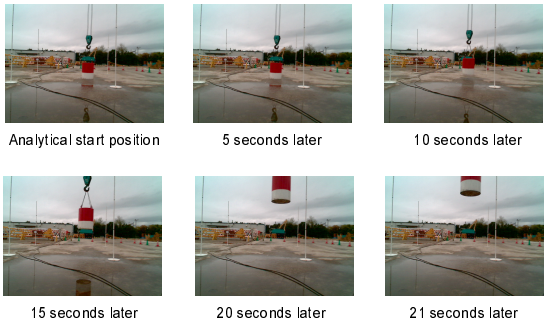

Fig. 35 Image of boom hoisting motion

object that was the admissible error was not able to be filled.

For this reason, it would appear that the target object in the camera image is slurred, because it was moving. And, the shutter timing of both cameras is not simultaneous.

Improving the program for shutter timing is the future tasks.

2.5 Application to Actual Crane

Here, the result of application to actual crane is described. In the experiment, the desk was set up in front of the crane and the stereo camera was put on it as shown in Fig.31.

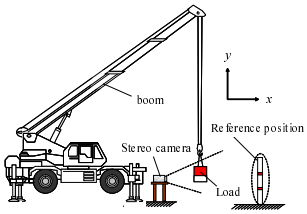

Fig. 31 Installation position of stereo camera

Fig. 32 Experiment scenery

The camera image which crane was circling (left to right) was shown in Fig.33. And, the results of locus analysis by this stereo camera data were compared before calibration and after calibration. The result of the comparison is shown in Fig.33. The top of boom position is given by the voltage data.

As shown in Fig.34, analyzed result of after calibration is near top of boom. It is confirmed that calibration corrected the depth coordinates.

Next, the operation of boom hoisting was conducted. In a similar way, the stereo camera data and analysis result are shown as follows.

It is confirmed the utility of the proposal method from Figs.34 and 36.

3 MODELING OF HYDRAULIC CONTROL SYSTEM FOR MOBLILE CRANE

When the intelligent interface for operation support is made, first it is need to know input-output characteristics of a crane. In a hydraulic system, it is difficult to design to consider about each characteris-

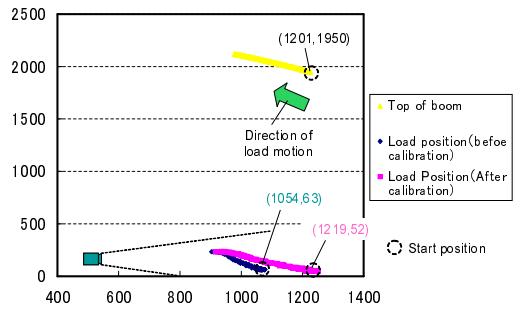

Fig. 36 Analyzed result of boom hoisting motion

tic, which have delay, characteristic of valve, dumping factor etc. So, it is considered separate static factor and dynamics factor. Here, the static hydraulic circuit model is described. Simple static hydraulic model is considered and it is identified output characteristics on actuator side considering engine rate and amount of lever. It doesn't contain dynamics factor. In the static hydraulic circuit model, key items are shown in the following equations.

Table. 2 Key parameter

	Symbol	Denomination
Flow Rate	Q	[L/min]
Pressure	P	[MPa]
Differential Pressure	ΔP	[MPa]
Open Space	A	[mm^2]
Displacement	q	[cm^3/rev]
Revolutions per Minute	N	[rpm]
Capacity Coefficient	c	
Density	γ	[kg/m^3]
Efficiency of Capacity	η	

※ Conversion of SI unit 1[kg/cm^2]=0.0981[MPa]

1. Expression of pressure drawdown ⋯ Orifice Equation

$$Q = c \times A \times \sqrt{(2 \times \Delta P) \div \gamma} \times 60 \qquad (22)$$

In general setting, c=0.63 and γ=870 equation (22) is described as follows;

$$Q = 1.8 \times A \times \sqrt{\Delta P} \qquad (23)$$

2. Amount of pump exhalation

$$Q = q \times N \times 10^{-3} \times \eta \qquad (24)$$

3. Rotational speed of motor The capacity of the motor on the load side and the efficiency of actuator are put with q_m and η_m;

$$N = Q \div q_m \times 10^3 \times \eta_m \qquad (25)$$

Valve-opening space is defined with the amount of lever stroke, and the flow rate of oil is proportional to engine rotational speed flows to the actuator. The known parameters and unknown parameters are given as follows.

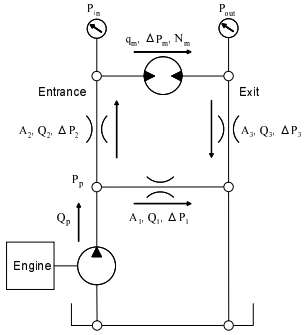

Fig. 37 Simple hydraulic circuit model

Known : $u,\ Q_p,\ A_1,\ A_2,\ A_3,\ \Delta P_m$
Unknown : $P_p,\ \Delta P_1,\ \Delta P_2,\ \Delta P_3,\ Q_1,\ Q_2,\ Q_3$

3.1 Operation of Boom Hoisting

The modeling of the operation of boom hoisting is discussed in this section.

3.1.1 Flow Rate and Pressure Relational Expression of Boom Hoisting Cylinder

Here, the relation between pumping rate and pressure in boom hoisting cylinder is evaluated from the orifice equation. Where, let Q_p be pumping rate adjacent engine, we find that

1. Flow rate relational expression

$$Q_p = Q_1 + Q_2 \qquad (26)$$

In boom hoisting circuit, we let S_2 be the pressure receiver dimension of cylinder head side and let Q_3 be the pressure receiver dimension of cylinder rodside. Because the amount of flow is decided inlet flow, the relation between S_2 and S_3

is different at rise and descent direction.

$$Q_3 = S_3/S_2 \times Q_2 \tag{27}$$
$$Q_3 = S_2/S_3 \times Q_2 \tag{28}$$

2. Relational expression between pressure and flow rate There are bleed-off circuit, meter-in and meter-out in speed control circuit of mobile crane. Let A_1 be bleed-off opening area and let A_2 be meter-in opening area and let A_3 be meter-out opening area. Then the following hold from orifis expression and orifice equation.

$$Q_1 = 1.8 \times A_1 \times\sqrt{\Delta P_1} \tag{29}$$
$$Q_2 = 1.8 \times A_2 \times\sqrt{\Delta P_2} \tag{30}$$
$$Q_3 = 1.8 \times A_3 \times\sqrt{\Delta P_3} \tag{31}$$

3.1.2 Pressure Expression of Boom Hoisting Cylinder at Rise

Let P_{in} be inlet pressure of the motor(head side pressure), let P_{out} be outlet pressure of the motor (rod side pressure), the load pressure of the motor is described as follows.

$$\Delta P_m = P_{in} - P_{out} \tag{32}$$

And, let P_p be pumping pressure, following equations are hold.

$$P_p = \Delta P_1 \tag{33}$$
$$P_p = \Delta P_2 + \Delta P_m + \Delta P_3 \tag{34}$$

From eqs.(26) to (34), method of simultaneous equations are hold to unknown number Q_2.

$$\left((A_1A_3)^2 + (A_1A_2)^2 \cdot \left(\frac{S_3}{S_2}\right)^2 - (A_2A_3)^2\right) {Q_2}^2 + \left(2{A_2}^2{A_3}^2Q_p\right) Q_2 + \Delta\ P_m(1.8A_1A_2A_3)^2 - (A_2A_3Q_p)^2 = 0 \tag{35}$$

In cylinder circuit, the output of actuator is not number of revolutions "N" but telescopic speed "V".
The cylinder speed at rise time is shown as follows.

$$V[\mathrm{cm/sec}] = Q_2[\mathrm{L/min}] \times 1000 \div 60 \div S_2[\mathrm{cm}^2] \tag{36}$$

3.1.3 Pressure Expression of Boom Hoisting Cylinder at Descent

At descent time, the pressure relational expression is different from at rise time because of work of the counter balance valve. The counter balance valve add back pressure on cylinder to prevent free fall. The spring is used for this back pressure. Let P_{in} be the spring force of the counter balance valve, equation (34) is shown as follows.

$$P_p = \Delta P_2 + P_{in} \tag{37}$$

It doesn't depend on meter-out and weight of hanging load. Thus, following equation is hold.

$$({A_1}^2{A_2}^2){Q_2}^2 + 2(Q_p{A_2}^2)Q_2 - {A_2}^2{Q_p}^2 + (1.8A_1A_2)^2 P_{in} = 0 \tag{38}$$

The cylinder speed at descent time is shown as follows.

$$V[\mathrm{cm/sec}] = Q_2[\mathrm{L/min}] \times 1000 \div 60 \div S_3[\mathrm{cm}^2] \tag{39}$$

3.1.4 Numerical Experiment

Here, numerical experiment is conducted by boom hoisting model discussed above. In this numerical experiment, the experiment data was used for the amount of the input. In the experiment of boom hoisting operation, each voltage data, boom hoisting lever, engine rotation, head pressure and rod pressure of cylinder etc, which are converted to physical quantity. Numerical experiment is conducted with these data as an input value. And, the simulation data is compared with experimental result.

The result of numerical experiment (simulation result) of boom hoisting operation and experiment data is shown as follows. The pump capacity is set $q = 35.5[\mathrm{cm}^3/\mathrm{rev}]$ and the capacity efficiency of pump is set $\eta = 0.94$.

From the result of numerical experiment, the simulation data is almost the same value with experiment data. But, the delay is slightly observed between simulation data and experiment data. This is because it doesn't consider dead time component. The dead time component is the time which signal is transmitted, so it is the time that oil flows to the actuator. It will be important an issue in the future.

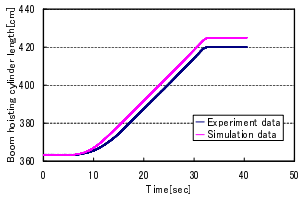

Fig. 38 Numerical experiment of boom hoisting at rise

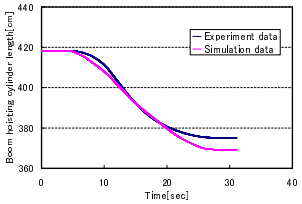

Fig. 39 Numerical experiment of boom hoisting at descent

3.2 Operation of Load Hoisting and Lowering

In operation of load hoisting and lowering, flow control valve is installed in the circuit to prevent the change of output characteristic by load weight. Load is hoisted and lowered by rolling of winch part. In this section, we describe about winch circuit and inspected simulation.

3.2.1 Flow Control Valve

Flow control valve is a valve that supplies flow rate corresponding to valve-opening area regardless of the load. The basic characteristic equation will be shown as follows. Variables in equation are as follows.

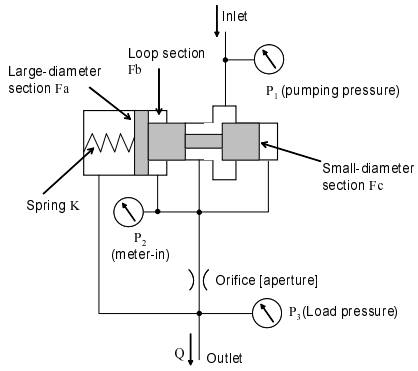

Fig. 40 Example of flow control valve diagram

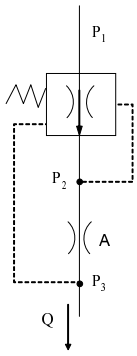

Fig. 41 Hydraulic circuit code

K : Spring force act on pressure compensated valve
F_a : Left side area of pressure compensated valve
F_b : Loop section area of right side of pressure compensated valve
F_c : Small-diameter area of right side of pressure compensated valve

From Fig.40, assuming that $F_a = F_b + F_c$, we get

$$P_2(F_b + F_c) = P_3F_a + K \quad (40)$$
$$F_a(P_2 - P_3) = K \quad (41)$$
$$P_2 - P_3 = K/F_a \quad (42)$$

Because spring modulus K is constant, the anteroposterior differential pressure $(P_2 - P_3)$ in orifice(aperture) adjust the flow control to keep it constant. Thus, the anteroposterior differential pressure is constant, the control flow rate dependeds on opening area of rifice(aperture).

3.2.2 Opening Aea in Equivalent Circuit Considered Flow Control Valve

The flow control valve of the crane used by the research is a little different from common it. It is designed to keep constant differential pressure of meter-in and the upstream part of flow control valve. For this reason, it is necessary to consider equivalent circuit model where flow control valve and meter-in were unified.

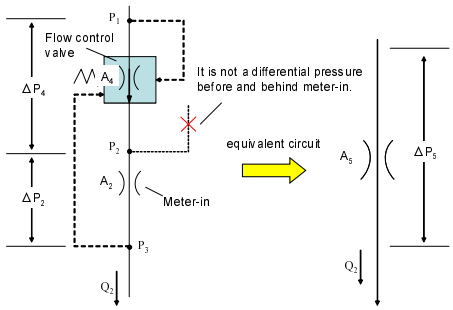

Fig. 42 Hydraulic circuit diagram in the flow control valve

Q_2 : Flow rate
P_1 : Inlet pressure
P_2 : Indoor pressure of pressure compensated valve
P_3 : Exit pressure
A_2 : Meter-in opening area
A_4 : Flow control valve opening area
A_5 : Valve-opening area of equivalent circuit
ΔP_2 : Meter-in differential pressure
ΔP_4 : Flow control valve differential pressure
ΔP_5 : Equivalent circuit differential pressure

From Fig.42, the flow rate which flows to equivalent circuit, meter-in and flow control valve is the same.

The following expressions are hold.

$$Q_2 = 1.8 \times A_2 \times\sqrt{\Delta P_2} \tag{43}$$
$$Q_2 = 1.8 \times A_4 \times\sqrt{\Delta P_4} \tag{44}$$
$$Q_2 = 1.8 \times A_5 \times\sqrt{\Delta P_5} \tag{45}$$

And, the differential pressure of the equivalent circuit is combination of the differential pressure caused in each valve.

$$\Delta P_5 = \Delta P_2 + \Delta P_4 \tag{46}$$

Thus, the opening area of equivalent circuit A_5 are desired from eqs.(43) to (46).

$$A_5 = \frac{A_2 A_4}{\sqrt{{A_2}^2 + {A_4}^2}} \tag{47}$$

3.2.3 Pressure Expression of Operation of Load Hoisting and Lowering

From the design, each valve-opening area of meter-in and flow control valve and their differential pressure are determined act on the amount of the lever operation. From equation (47), the opening area of equivalent circuit is evaluated and is substituted into equation (45). So, it has nothing to do with pumping rate and load weight, it depends on only an amount of lever operation.

3.2.4 Numerical Experiment

As well as the numerical experiment of boom hoisting, the experimental data was used for the amount of the input. In the same way, the pump capacity is set $q = 35.5[\mathrm{cm}^3/\mathrm{rev}]$, the capacity efficiency of pump is set $qm = 53.5[\mathrm{cm}^3/\mathrm{rev}]$. Furthermore , motor capacity is set $qm = 53.5[\mathrm{cm}^3/\mathrm{rev}]$, the capacity efficiency of motor is set $\eta_m = 0.95$, axle ratio of winch is set i_G=20.0. Because it is a winch single rotation experiment, the number of pumps is assumed to be 2 pieces.

From the result of numerical experiment, the simulation data is almost the same value with the experiment data. But, the delay is slightly observed between the simulation data and the experiment data similarly with that in the boom hoisting operation.

4 INTELLIGENT INTERFACE SYSTEM

Let consider the image of intelligent interface system for crane operation support as shown in Fig.44.

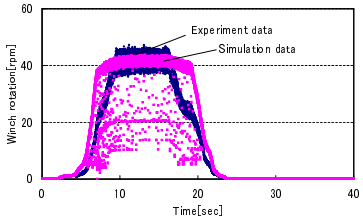

Fig. 43 Simulation result of the operation of winch rotation

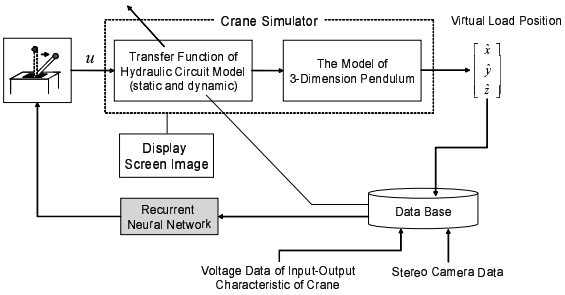

Fig. 44 Image of intelligent interface for operation support

Almost all of crane operators operate crane seeing the load. Expert persons operate the lever under prediction. To make the human model (human interface), crane simulator is designed. In Fig.44, u is an amount of operation and $\hat{x}, \hat{y}, \hat{z}$ are virtual load position. Simulation data and experimental data are stored in data base. Experimental data are crane input-output characteristic data and load position data. Virtual data given by crane simulator is stored in data base. Data stored in data base are needed to learn by neural network model to extracted the amount of characteristics. Neural network model already learned is need to determine the amount of operation. The display screen image is role of displaying human by visual information processing, and the neural network model acts as the human brain. Crane input-output data correspond to the amounts of lever and controll variables (boom angle, angle rate $\cdots$) are collected as voltage data with LabVIEW system. At the same time, load position data is measured with stereo camera method.

The experimental condition of actual crane is shown in Fig.45. Sensor♯1 is for voltage data of crane input-output with LabVIEW and Sensor♯2 is for load position data with stereo camera. The example of the application of stereo camera for actual crane is shown

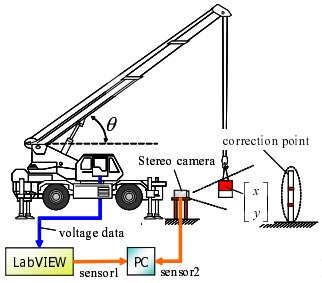

Fig. 45 Experiment condition

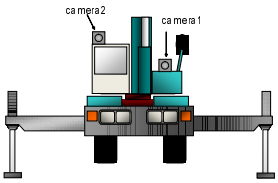

Fig. 46 Example of the application of stereo camera for actual crane

in Fig.46.

Each data acquired in the experiment is shown as follows. Data in Fig.47 is one example of the volatge data when crane boom is hosisted and the corresponding stereo camera data is shown in Fig.48.

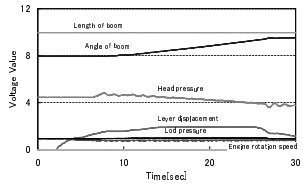

Fig. 47 Voltage data of crane operating

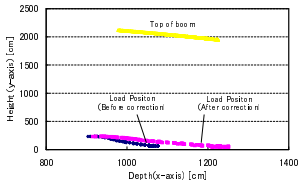

Fig. 48 Load position data by stereo camera

This human interface system is that stereo camera detecting load position and it is add to the amount of the input as amount of correction to inhibit swinging of the hanging load when a hanging load swings widely by the disturbance of gust and inertia force, etc. So, when a hanging load swings by disturbance, some errors are observed between simulation data and stereo data. At this time, an amount of correction is generated. This purpose is to leave the operation person's preference to some extent. For this reason, in the case the hanging load position measured with stereo camera is far from simulation data and it is greatly different from the human model of expert person which is learned by neural network, the amount of the correction is to be generated. This function will be able to operate expert level. Consequently, it will lead to the decreasing of the number of crane accidents.

5 CONCLUSION

In this research, we are aiming at the development of the human support system of crane operation. This time, the measurement system used the stereo method with two cameras was constructed for the acquisition of hanging load positional data. Furthermore, the modeling of the crane characteristic is made and the simulation tests are run to collect data. In the case the stereo camera is applied for actual crane, it is difficult that the two cameras are set up accurately along axis of the coordinate. Moerover, it is not avoided to cause to a slight misalignment in the direction of the camera by a change with the passage of time and the vibration, etc.

In this research, the calibration technology was researched focused on the error of the installation of the camera and the error in the installation position.

In the development, the misalignment of the angle of the camera and installation position are detected by the optimization technique with the coordinate of the reference point that three dimension position determined beforehand and the measurements were made with the stereo camera method. The object which is hanging load was fixed and the analysis was conducted to confirm utility of the proposal method. As the result, it was confirmed that the measuring error fell within about 2 percent.

Next, the simulation which is the operation of boom hoisting and load hoisting and lowering by (winch rotation) is conducted. From the results of the numeric experiment, it was known that the simulation data is almost the same value with the experiment data. But, the delay was slightly observed between simulation and experiment data. The reason was that it doesn't consider dead time component. The dead time component is the time a signal is transmitted, so it is time that oil flows to the actuator.

In the future works, this delay is to be treated assuming dead time component and first order delay as the transfer function. The parameters of the assumed transfer function are to be identified by the optimization algorithm.

REFERENCES

[1] A. Nakazumi, T. Inoue, K. Fukushima, H. Kinukawa: *Report of Kobe Steel, Ltd.*, Vol. 37, No. 4, pp. 41-44 (1987).

[2] M. Anabuki, K. Shimada, H. Hirata: *Bulletin in department of technology from Tokai university*, Vol. 40, No. 1 (2000).

[3] K. Hashimoto: *Workshop of Day Before Rally of Control Section*, (2001), pp.37-68.

[4] M. Akiyama: Photo survey, Sankaido (2001).

[5] T. Abe, M. Koike, T. Kozyo, M. Shimizu, M, Tuzuki: Introduction to numerical analysis, Syoukoudo (1992).

[6] Y. Sakai: Introduction to digital image processing , CQ Publishing (2002).

[7] Shmuel Peleg et al: *IEE International Conference*, Vol. 1, (2000), pp. 208-214.

[8] Won S. Kim, et al: *IEE International Conference*, Vol. 1, (2005), pp. 1409-1416.

[9] N. Kobayashi, et al: Verity of robotic control, Korona Publishing (1997).

[10] M. Yanagiura, T. Ibaraki: Combinational optimization, Asakura bookstore (2001).

[11] K. Nishikawa, N. Sannomiya, T. Ibaraki: Optimization, Iwanami bookstore (1999).

[12] Edited by Robert Azencott: Simulated Annealing ; parallelization Techniques, John Wiley and Sons (1992).

[13] E. H. L. Aarts and J. H. M. Korst: Simulated Annealing and Boltzman Machines, John Wiley and Sons (1989).

[14] T. Sakamoto, K. Miki: Read and Draw ～Oil Pressure / Pneumatic Circuit Diagram～Ohm Publishing (2003).

[15] J. J. Hopfield: Neurons with graded response have collective computational properties like those of two-state neurons, Proc. Nat. Acad. Sci. USA. 81, (1984), pp.3088-3092.